

## MALDI–TOF MS Study of Aromatic Polybenzoxazole Fibers

Anthony P. Gies\* and David M. Hercules

Department of Chemistry, Vanderbilt University, Nashville, Tennessee 37235

Received January 6, 2006; Revised Manuscript Received February 8, 2006

**ABSTRACT:** The evaporation-grinding MALDI–TOF MS sample preparation method and evolved gas analysis/GC/MS (EGA/GC/MS) were used to study the cyclodehydration of polybenzoxazole and poly(benzoxazoleamide) precursors. Precursor fibers were heated from 100 to 300 °C while evolved gases were monitored by GC/MS; after each heating, samples were removed for MALDI–TOF MS analysis. Changes observed in MALDI–TOF mass spectra result from cyclodehydration, along with end group, and structure modifications (due to decarboxylation and branching). Evolved gas analysis/GC/MS and thermogravimetric analysis data indicate mass loss (from chain rupture) and evolution of low mass material which lead to branching. Cured polybenzoxazole fibers display an overall predominance of branched species with minor reduction in molecular weight whereas cured poly(benzoxazoleamide) fibers yield linear species as the predominant product with only minor branching observed and significant reductions in molecular weight. Results from this study indicate that a combination of MALDI–TOF MS and EGA/GC/MS has great potential for examination of thermal, chemical, and photodegradation pathways of high molecular weight, condensation polymers.

## Introduction

Major advances in the theory, synthesis, and processing of rigid polymers in the past 30 years have raised polybenzoxazoles (PBOs) from the status of obscure laboratory curiosities to a new class of environmentally resistant, high strength, high modulus materials, receiving much attention from both the academic and industrial communities. Polybenzoxazoles are aromatic heterocyclic polymers that belong to a group of rigid-rod polymers first introduced in the 1960s and further developed in the 1980s by SRI International under the U.S. Air Force Ordered Polymers Research Program, to match the thermal stability requirements of the aerospace industry.<sup>1</sup>

Wholly aromatic PBOs offer superior chemical resistance, high fiber strength, and ultrahigh modulus along with being the most thermally and thermooxidatively stable organic polymers known.<sup>2</sup> However, uses of wholly aromatic PBOs have been limited because they are generally insoluble in most solvents (except for strong acids), possess high glass transition temperatures, and decompose below their melting points.<sup>3</sup> Despite these limitations, their outstanding properties have been the driving force to investigate their use in fibers, films, coatings, and composites, as well as ballistic-protection fabrics and panels, because of the high energy absorption and rapid dissipation of impact by the fibrillar morphology.<sup>3</sup>

Conventional methods of analysis (i.e., viscometry, titration, TGA, DSC, DMA, GPC, NMR, IR, Py-GC/MS)<sup>1,4,5</sup> have proven to be inadequate in providing exhaustive information on the molecular mass distribution, chemical distribution, and structural heterogeneities present in these fibers.<sup>6</sup> This is due to weak signals generated from the low concentrations of end groups and byproducts with respect to the polymer backbone. Background noise often masks these weak signals preventing their detection and hence they were seldom reported in the past.<sup>7</sup> However, MALDI–TOF MS provides the mass accuracy and resolution for direct structural determination of the species and end groups present in a complex polymeric sample.<sup>6</sup>

Recent studies investigating PBO resistance to acid chemical

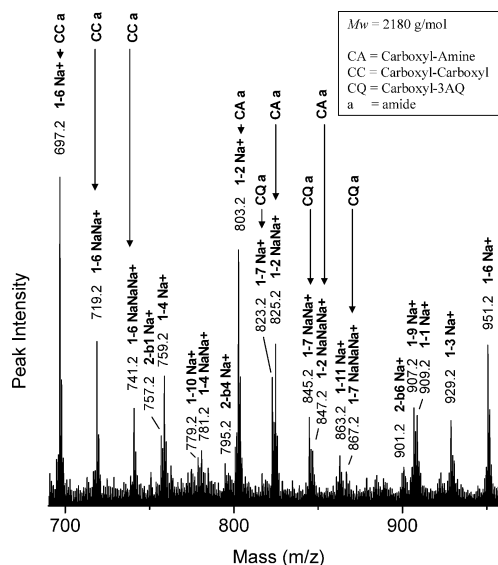


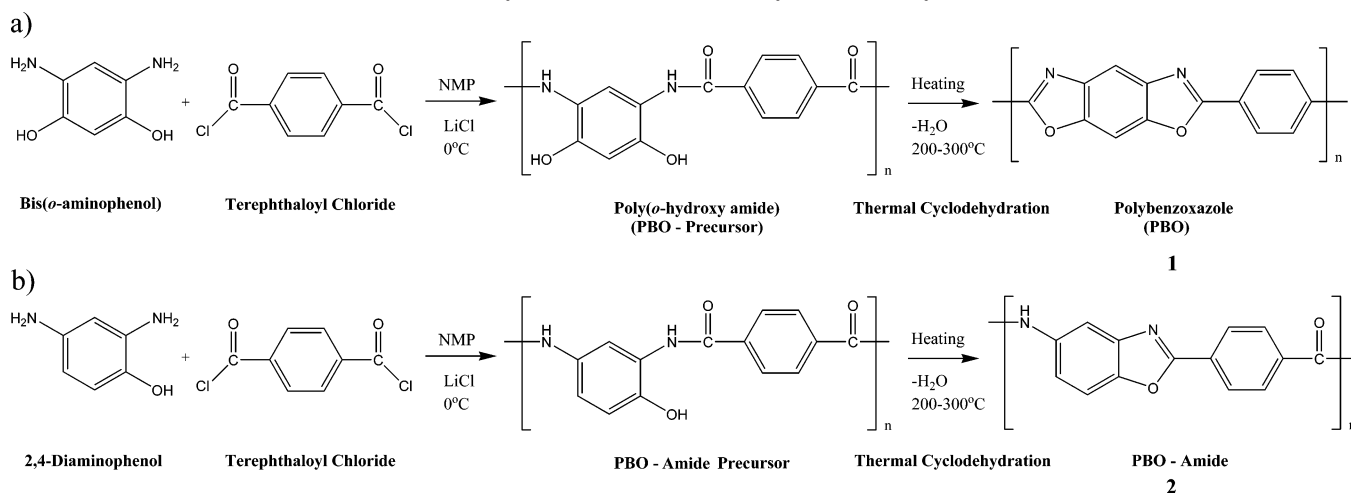
**Figure 1.** MALDI–TOF mass spectrum (covering one repeat unit, 690–960 Da) of PBO–amide precursor fibers. Sample prepared by the E–G method in 3AQ and cationized with NaTFA.

attack and UV irradiation, which raised questions of PBO reliability as protective apparel, have launched further investigations throughout U.S. Government laboratories.<sup>8</sup> In an effort to substantiate or refute claims of PBO failure due to degradation, our laboratory is currently developing methods of analysis for PBO fibers with the ultimate goal of identifying sources of PBO chain rupture and to link these sources to identifiable degradation products.

In the present study, we present our initial results which exploit the evaporation-grinding MALDI–TOF MS sample preparation method<sup>9–11</sup> and evolved gas analysis/GC/MS (EGA/GC/MS) to examine the thermal curing of poly(*o*-hydroxy amide) (PAOH) and a poly(benzoxazoleamide) precursor. By following the curing process from 100 to 300 °C, we were able to identify critical temperatures in the cyclodehydration process that lead to structural, distribution, and end group changes. This work indicates that MALDI–TOF MS has great potential for

\* Corresponding author. Telephone: (615) 343-5980. E-mail: a.gies@vanderbilt.edu.

## Scheme 1. Polybenzoxazoleamide and Polybenzoxazole Synthesis



examination of degradation processes of PBO fibers and other condensation polymers. Studies are currently underway to validate this proposal.

## Experimental Section

**Solution Polymerization of Poly(*o*-hydroxy amide) Fibers.** Poly(*o*-hydroxy amide) fibers were synthesized via solution polymerization.<sup>1</sup> All reagents were obtained from commercial sources and used as received after analysis by Py-GC/MS to verify their purity. Finely ground (and dried) lithium chloride (0.2 g) and 140.0 mL of dry 1-methyl-2-pyrrolidinone (NMP, Fisher) were added to a well-dried, 250 mL three necked flask, with nitrogen inlet/outlets and magnetic stirrers. To this suspension, 5.8 g (27.3 mmol) of powered 4,6-diaminoresorcinol dihydrochloride (Aldrich), and 8.9 mL (109.2 mmol) of pyridine (Aldrich) were added with stirring. The resulting mixture was cooled to 0 °C. Subsequently, with continued cooling and rigorous stirring, 5.5 g (27.3 mmol) of terephthaloyl chloride (Aldrich) were added to the mixture. Stirring was continued for 45 min at 0 °C under a nitrogen atmosphere. The resulting viscous solution was terminated with large volumes of distilled water or ethanol yielding a fibrous precipitate. Each precipitate was filtered and washed thoroughly with the appropriate terminating solution then dried at room temperature for 72 h in a

vacuum. The experimental conditions (i.e., NMP as the solvent) were chosen to ensure that the reactions would yield low molecular weight PAOH fibers.<sup>1</sup> The two functions of an aminophenol could be acylated. However, *N*-acylation forms the more stable isomer vs *O*-acylation.<sup>12</sup> Further complicating the synthesis, is the issue of *N*-monoacylation vs diacylation which Sillion et al.<sup>12</sup> solved by performing the condensation reaction in the presence of an inorganic salt (LiCl) in NMP to favor the *N*-monoacylated product, hence the use of LiCl in our synthesis. The structures of the oligomers were assumed to be as shown in Scheme 1a.

**Solution Polymerization of Poly(benzoxazoleamide) Precursor Fibers.** Poly(benzoxazoleamide) precursor fibers were synthesized via solution polymerization.<sup>1</sup> All reagents were obtained from commercial sources and used as received after analysis by Py-GC/MS to verify their purity. To a well-dried, 250 mL three necked flask, with nitrogen inlet/outlets and magnetic stirrers, 0.2 g of finely ground (and dried) lithium chloride and 140.0 mL of dry 1-methyl-2-pyrrolidinone (NMP, Fisher) were added. To this suspension, 5.4 g (27.3 mmol) of powered 4,6-diaminophenol dihydrochloride (Aldrich), and 8.9 mL (109.2 mmol) of pyridine (Aldrich) were added with stirring. The resulting mixture was cooled to 0 °C. Subsequently, with continued cooling and rigorous stirring 5.5 g (27.3 mmol) of terephthaloyl chloride (Aldrich) were added to the mixture. Stirring was continued for 45 min at 0 °C under a nitrogen

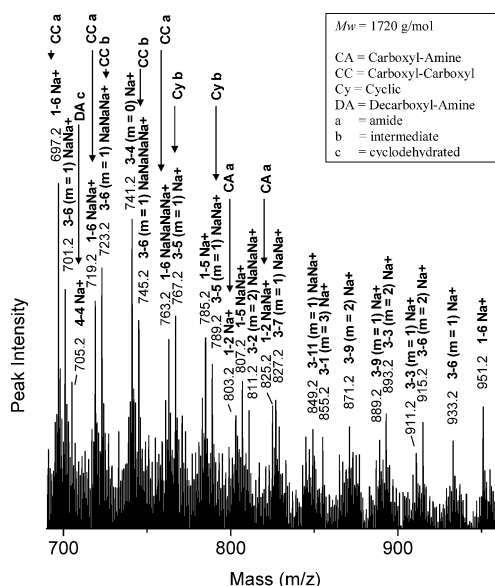


**Figure 2.** MALDI-TOF mass spectrum (covering one repeat unit, 690–960 Da) of PBO-amide precursor fibers after heat treatment at 250 °C for 45 min. Sample prepared by the E-G method in 3AQ and cationized with NaTFA.

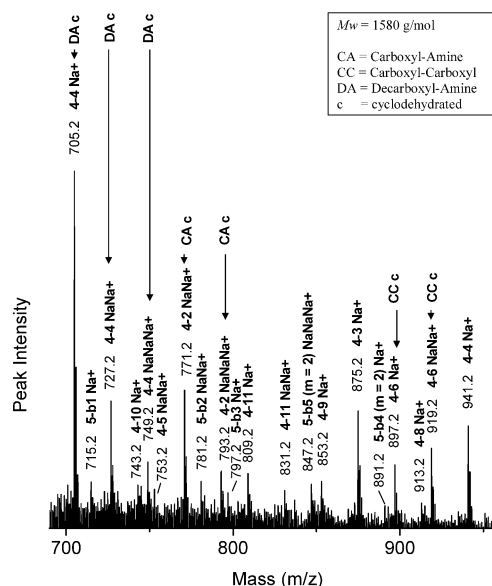


**Figure 3.** MALDI-TOF mass spectrum (covering one repeat unit, 690–960 Da) of PBO-amide precursor fibers after heat treatment at 300 °C for 45 min. Sample prepared by the E-G method in 3AQ and cationized with NaTFA.

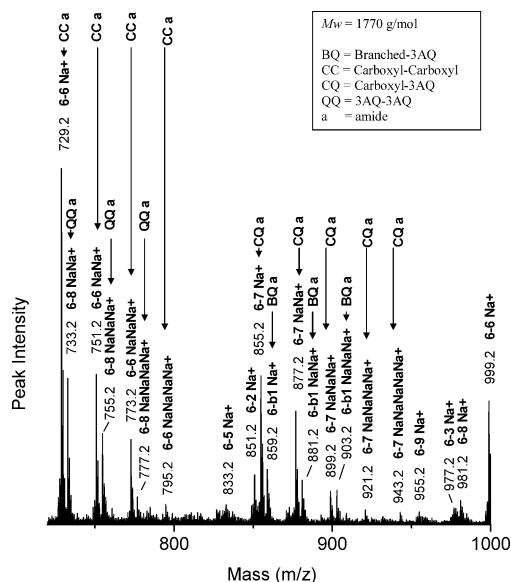


**Figure 4.** MALDI-TOF mass spectrum (covering one repeat unit, 720–1000 Da) of PBO precursor fibers. Sample prepared by the E-G method in 3AQ and cationized with NaTFA.

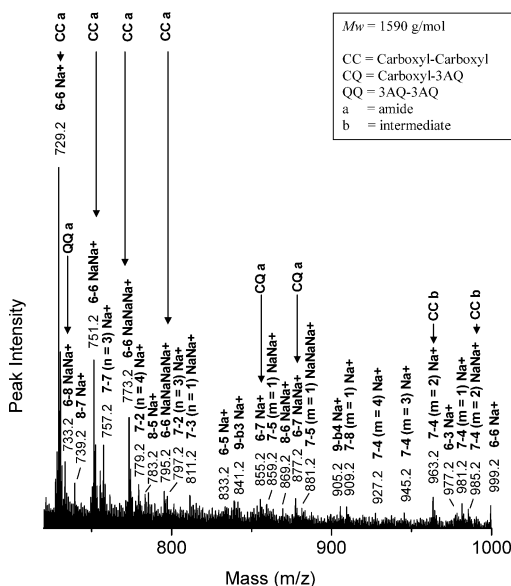


**Figure 5.** MALDI-TOF mass spectrum (covering one repeat unit, 720–1000 Da) of PBO precursor fibers after heat treatment at 250 °C for 45 min. Sample prepared by the E-G method in 3AQ and cationized with NaTFA.

atmosphere. The resulting viscous solution was terminated with large volumes of distilled water or ethanol yielding a fibrous precipitate. Each precipitate was filtered and washed thoroughly with the appropriate terminating solution then dried at room temperature for 72 h in a vacuum. The structures of the oligomers were assumed to be as shown in Scheme 1b.

**MALDI-TOF MS Measurements.** All fibers were analyzed using a Voyager Elite DE STR MALDI-TOF MS (Applied Biosystems, Framingham, MA) equipped with a 337 nm  $N_2$  laser. All spectra were obtained in the positive ion mode using an accelerating voltage of 20 kV and a laser intensity of  $\sim 10\%$  greater than threshold. The grid voltage, guide wire voltage, and delay time were optimized for each spectrum to achieve the best signal-to-noise ratio. All spectra were acquired in the reflectron mode with a mass resolution greater than 3000 fwhm; isotopic resolution was observed throughout the entire mass range detected. External mass calibration was performed using protein standards from a Sequazyme Peptide Mass Standard Kit (Applied Biosystems) and a three-point calibration method using Angiotensin I ( $m = 1296.69$

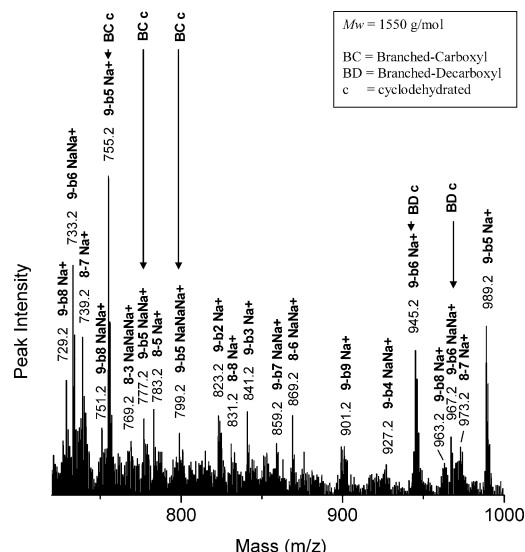


**Figure 6.** MALDI-TOF mass spectrum (covering one repeat unit, 720–1000 Da) of PBO precursor fibers after heat treatment at 300 °C for 45 min. Sample prepared by the E-G method in 3AQ and cationized with NaTFA.

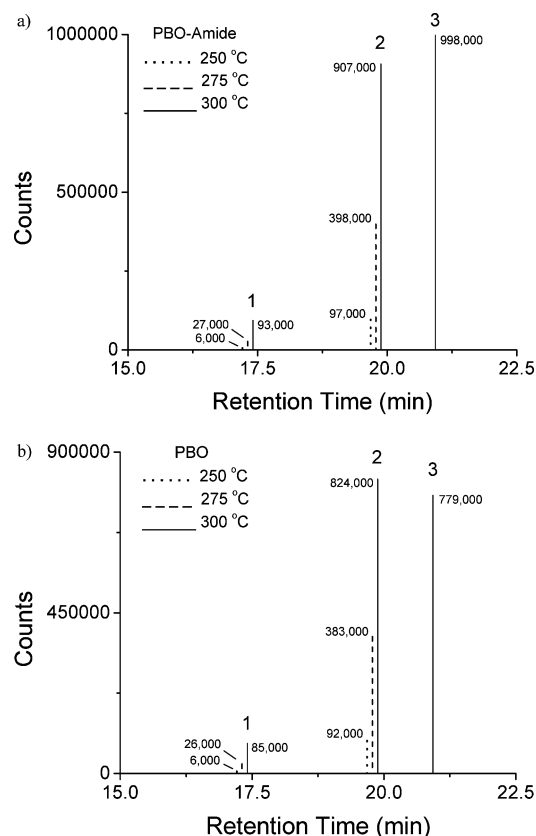


**Figure 7.** Representative peak intensities extracted from EGA/GC/MS chromatograms of PBO-amide and PBO precursor fibers cured between 100 and 300 °C.

Da), ACTH (clip 1–17) ( $m = 2093.09$  Da), and ACTH (clip 18–39) ( $m = 2465.20$  Da). Internal mass calibration was subsequently performed using a PEG standard (Polymer Source, Inc.) to yield monoisotopic masses exhibiting a mass accuracy better than  $\Delta m = \pm 0.1$  Da. The instrument was calibrated before every measurement to ensure constant experimental conditions. All samples were run in 3-aminoquinoline (3AQ, Aldrich) doped with sodium trifluoroacetate (NaTFA, Aldrich), potassium trifluoroacetate (KTFA, Aldrich), or cesium trifluoroacetate (CsTFA, Aldrich). All spectra displayed the expected mass shifts for the

Table 1. Structural Assignments for Peaks in the MALDI-TOF Mass Spectra Reported in Figures 1 and 2<sup>a</sup>

Species	Structure (M)	No Heat Na <sup>+</sup> M (Da)	250 °C Na <sup>+</sup> M (Da)
1-1		655.2 (n = 2), <u>909.2</u> (n = 3)... 4214.2 (n = 16)	655.2 (n = 2), <u>909.2</u> (n = 3)... 1672.5 (n = 6)
1-2		549.1 (n = 2), <u>803.2</u> (n = 3)... 4362.2 (n = 17)	549.1 (n = 2), <u>803.2</u> (n = 3)... 1820.5 (n = 7)
1-3		675.2 (n = 2), <u>929.2</u> (n = 3)... 4234.2 (n = 16)	675.2 (n = 2), <u>929.2</u> (n = 3)... 1437.4 (n = 5)
1-4		505.2 (n = 1), <u>759.2</u> (n = 2)... 4064.1 (n = 15)	505.2 (n = 1), <u>759.2</u> (n = 2)... 1521.4 (n = 5)
1-5		531.1 (n = 2), <u>785.2</u> (n = 3)... 3836.0 (n = 15)	531.1 (n = 2), <u>785.2</u> (n = 3)... 1802.5 (n = 7)
1-6		697.2 (n = 2)... <u>4256.1</u> (n = 16)	697.2 (n = 2)... 1714.4 (n = 6)
1-7		569.1 (n = 1), <u>823.2</u> (n = 2)... 4128.1 (n = 15)	569.1 (n = 1), <u>823.2</u> (n = 2)... 1840.5 (n = 6)
1-8		695.2 (n = 1)... <u>4000.1</u> (n = 14)	695.2 (n = 1)... 1203.3 (n = 3)
1-9		653.2 (n = 2), <u>907.2</u> (n = 3)... 3449.9 (n = 13)	653.2 (n = 2), <u>907.2</u> (n = 3)... 1415.4 (n = 5)
1-10		525.2 (n = 1), <u>779.2</u> (n = 2)... 2304.6 (n = 8)	525.2 (n = 1), <u>779.2</u> (n = 2)... 1287.4 (n = 4)
1-11		609.2 (n = 1), <u>863.2</u> (n = 2)... 3406.0 (n = 12)	609.2 (n = 1), <u>863.2</u> (n = 2)... 1117.3 (n = 3)

<sup>a</sup> Right-hand columns display mass ranges of the indicated species at different curing temperatures. Underlined masses correspond to the lowest mass peaks in the figures.

respective cationizing agent and were used for spectral interpretation. However, NaTFA was the reagent of choice since it yielded spectra with the greatest S/N ratios. Attempts were made to obtain MALDI-TOF mass spectra using silver and copper salts; however, we were unable to obtain usable mass spectra using these cationizing agents. Additional attempts were made to obtain mass spectra in the negative ion mode but they too were unsuccessful. The samples were prepared using the evaporation-grinding method (E-G method)<sup>9-11</sup> in which a 2 mg sample of aromatic fiber was ground to a fine powder using an agate mortar and pestle. Then molar ratios (with respect to the moles of polymer) of 25 parts matrix and one part cationizing agent (NaTFA, KTFA, or CsTFA) were added to the finely ground polymer along with 60  $\mu$ L of distilled tetrahy-

drofuran (THF, Fisher). The mixture was ground until the THF evaporated after which the residue that accumulated on the sides of the mortar was pushed down to the bottom of the vessel. The mixture was then ground again to ensure homogeneity. A sample of the mixture was then pressed into a sample well by spatula on the MALDI sample plate. The weight-averaged molecular weights ( $M_w$ ) of all fibers were determined with the software supplied by the manufacturer of our MALDI-TOF MS.

**EGA/GC/MS Measurements.** All fibers were analyzed using a Frontier Labs double-shot pyrolyzer (Frontier Labs, Japan) interfaced to a Hewlett-Packard 5890 II gas chromatograph and a Hewlett-Packard 5970 mass selective detector. Platinum cups were used to ensure homogeneous heating of the sample. Evolved gas

Table 2. Structural Assignments for Peaks in the MALDI–TOF Mass Spectra Reported in Figures 1 and 2<sup>a</sup>

Species	Structure (M)	No Heat Na <sup>+</sup> M (Da)	250 °C Na <sup>+</sup> M (Da)
2-b1		<u>503.1</u> (n = 0), <u>757.2</u> (n = 1)... 3044.8 (n = 10)	<u>503.1</u> (n = 0), <u>757.2</u> (n = 1)... 1011.2 (n = 2)
2-b2		<u>713.2</u> (n = 1)... 1984.6 (n = 6)	<u>713.2</u> (n = 1)... 967.3 (n = 2)
2-b3		<u>817.2</u> (n = 0)... 2088.6 (n = 5)	<u>817.2</u> (n = 0)... 1071.3 (n = 1)
2-b4		<u>795.2</u> (n = 0)... 3082.8 (n = 9)	<u>795.2</u> (n = 0)... 1303.3 (n = 2)
2-b5		<u>559.1</u> (n = 0), <u>813.2</u> (n = 1)... 2592.7 (n = 8)	<u>559.1</u> (n = 0), <u>813.2</u> (n = 1)... 813.2 (n = 1)
2-b6		<u>901.1</u> (n = 0)... 3188.8 (n = 9)	

<sup>a</sup> Right-hand columns have the same information as Table 1.

analysis was performed using the following protocol: 50 mg of precursor fiber was placed into a platinum sample cup and allowed to purge under a 100 mL/min flow of 99.999% pure (grade 5) helium for 3 min inside the pyrolyzer. The pyrolyzer was then heated to 100 °C, and a GC/MS was taken of the evolved gases. After obtaining the GC/MS, the sample was briefly removed from the pyrolyzer furnace, and the furnace temperature raised 25 °C. This procedure was repeated until a temperature of 300 °C was completed by the GC/MS. The GC/MS used a heating program starting at 50 °C for 2 min and ramping at 12.5 °C for 20 min before finally holding at 300 °C for 8 min, for a total GC/MS heating cycle of 30 min. A 99/1 split of the carrier gas was used to ensure that the gases were introduced as a “plug” and not to corrupt the mass spectrometer.

The pyrolyzer was also used to cyclodehydrate the precursor fibers for MALDI–TOF MS analysis. Fifty mg of precursor fiber were placed in a platinum sample cup and allowed to purge under a 100 mL/min stream of grade 5 helium gas. The sample cup was introduced into the furnace at a temperature of 100 °C and maintained at that temperature for 30 min. After this time interval had expired the platinum cup was removed from the pyrolyzer, and a 2 mg sample of polymer was analyzed by MALDI–TOF MS. The platinum cup was then suspended in a sealed chamber above the furnace in a 100 mL/min stream of grade 5 helium for 3 min before being introduced into the furnace that was set at 25 °C higher than the last heating temperature and reheated for 30 min. This procedure was repeated until a 300 °C heating interval was completed.

## Results and Discussion

In an effort to determine the effectiveness of MALDI–TOF MS for the analysis of PBO fibers, PBO and PBO–amide precursors were synthesized to examine their cyclodehydration

with a combination of MALDI–TOF MS and EGA/GC/MS. It was envisioned that MALDI–TOF mass spectra (with respect to the temperature at which the precursor was cured) would reveal amide, intermediate amide/benzoxazole, and fully cured benzoxazole species.

Changes observed in the MALDI–TOF mass spectra result from cyclodehydration, along with the end group, and structure modifications (due to decarboxylation and branching). It should also be pointed out that all figures display peak splitting due to hydrogen/sodium exchange, which is a phenomenon associated with analyzing these materials by the E–G method. Moreover, the main peaks in all figures are labeled with peak series (resulting from hydrogen/sodium exchange) to simplify figure comparison and emphasize changes occurring between the figures. Figures 1–3 show expanded regions (690–960 Da) of the resulting PBO–amide precursor spectra, and Figures 4–6 show expanded regions (720–1000 Da) of the resulting PBO precursor spectra under various heating conditions. Figures 1–6 show peaks labeled in the *x*–*y* format (*x* = table number, *y* = structure number) followed by the atom and/or ion which has been added to the oligomers during the MALDI process. For instance, a peak labeled 1–6 NaNa<sup>+</sup> corresponds to a structure found in Table 1, structure 6, in which a sodium ion has been exchanged for a hydrogen ion and is ionized by an additional sodium ion from the MALDI process. For easier peak identification, all mass spectra which display branched species are labeled with the letter “b” in front of their structure number (example: 2-b1 Na<sup>+</sup>). Tables 1–9 show mass ranges of all identified species from Figures 1–6 with underlined masses corresponding to the lowest mass peaks shown in the figures. The mass shifts observed in the MALDI spectra of the various



Table 3. Structural Assignments for Peaks in the MALDI-TOF Mass Spectra Reported in Figure 2<sup>a</sup>

Species	Structure (M)	250 °C Na <sup>+</sup> M (Da)
3-1		637.2 (n = 1, m = 1), 891.2 (n = 2, m = 1)... 1145.3 (n = 3, m = 1) 619.2 (n = 1, m = 2), 873.2 (n = 2, m = 2)... 1127.3 (n = 3, m = 2) 601.2 (n = 1, m = 3), 855.2 (n = 2, m = 3)... 1872.5 (n = 6, m = 3)
3-2		531.1 (n = 1, m = 1), 785.2 (n = 2, m = 1)... 1802.5 (n = 6, m = 1) 513.1 (n = 1, m = 2), 767.2 (n = 2, m = 2)... 1784.5 (n = 6, m = 2)
3-3		657.2 (n = 1, m = 1), 911.2 (n = 2, m = 1)... 1674.5 (n = 5, m = 1) 893.3 (n = 2, m = 2)... 1656.5 (n = 5, m = 2)
3-4		741.2 (n = 1, m = 0)... 1758.5 (n = 5, m = 0)
3-5		767.2 (n = 2, m = 1)... 1784.5 (n = 6, m = 1)
3-6		679.1 (n = 1, m = 1), 933.2 (n = 2, m = 1)... 1696.4 (n = 5, m = 1) 661.1 (n = 1, m = 2), 915.2 (n = 2, m = 2)... 1678.4 (n = 5, m = 2)
3-7		805.2 (n = 1, m = 1)... 1822.5 (n = 5, m = 1)
3-8		931.3 (n = 1, m = 1)... 1694.5 (n = 4, m = 1)
3-9		635.2 (n = 1, m = 1), 889.2 (n = 2, m = 1)... 1906.5 (n = 6, m = 1) 871.2 (n = 2, m = 2)... 1888.5 (n = 6, m = 2)
3-10		761.2 (n = 1, m = 1)... 1269.4 (n = 3, m = 1)
3-11		845.2 (n = 1, m = 0)... 1099.3 (n = 2, m = 0) 827.2 (n = 1, m = 1)... 1357.4 (n = 3, m = 1)

<sup>a</sup> Right-hand column has the same information as Table 1

salt-doped and reaction-terminated solutions allowed unambiguous assignment of the isobaric peaks corresponding to the PBO-amine and PBO precursor oligomers.

Figure 1 displays a PBO-amine precursor mass spectrum ( $M_w = 2180$  g/mol) with three predominant series of species, labeled in order of abundance. Series CCA represents species which possess carboxyl-carboxyl end groups (species 1-6),

series CAa represents species possessing carboxyl-amine end groups (species 1-2), and series CQa identifies species resulting from carboxyl-carboxyl end group adduct formation with the 3AQ MALDI matrix (species 1-7). Less abundant species contain the following end groups: decarboxyl-carboxyl (species 1-9) and amine-amine (species 1-1) followed by decarboxyl-amine (species 1-4). This figure exhibits an overall predomi-

Table 4. Structural Assignments for Peaks in the MALDI-TOF Mass Spectra Reported in Figures 2 and 3<sup>a</sup>

Species	Structure (M)	250 °C Na <sup>+</sup> M (Da)	300 °C Na <sup>+</sup> M (Da)
4-1		619.2 (n = 1), 855.2 (n = 2)... 1800.5 (n = 7)	619.2 (n = 1), 855.2 (n = 2)... 1327.4 (n = 5)
4-2		513.1 (n = 2), 749.2 (n = 3)... 1221.3 (n = 5)	513.1 (n = 2), 749.2 (n = 3)... 2874.7 (n = 12)
4-3		639.2 (n = 2), 875.2 (n = 3)... 1820.5 (n = 7)	639.2 (n = 2), 875.2 (n = 3)... 2764.7 (n = 11)
4-4		705.2 (n = 2)... 1177.3 (n = 4)	705.2 (n = 2)... 2830.7 (n = 11)
4-5		731.2 (n = 2)... 1676.4 (n = 7)	731.2 (n = 2)... 2148.5 (n = 9)
4-6		661.1 (n = 2), 897.2 (n = 3)... 1369.3 (n = 5)	661.1 (n = 2), 897.2 (n = 3)... 2786.7 (n = 11)
4-7			551.1 (n = 1), 787.2 (n = 2)... 2912.7 (n = 11)
4-8		677.2 (n = 1), 913.2 (n = 2)... 1149.3 (n = 3)	677.2 (n = 1), 913.2 (n = 2)... 2802.7 (n = 10)
4-9		617.2 (n = 2), 853.2 (n = 3)... 1798.5 (n = 7)	617.2 (n = 2), 853.2 (n = 3)... 2742.7 (n = 11)
4-10		507.1 (n = 1), 743.2 (n = 2)... 1688.4 (n = 6)	507.1 (n = 1), 743.2 (n = 2)... 2868.7 (n = 11)
4-11		573.2 (n = 1), 809.2 (n = 2)... 1754.5 (n = 6)	573.2 (n = 1), 809.2 (n = 2)... 2934.8 (n = 11)

<sup>a</sup> Right-hand columns have the same information as Table 1.

nance of linear species with only minor quantities of cyclic (species 1–5) and branched species (Table 2) present. The abundances of the observed end groups are those expected for a synthesis using a very slight excess of diacid chloride monomer.

Figure 2 displays a PBO–amide precursor mass spectrum (after curing at 250 °C for 45 min) ( $M_w = 1720$  g/mol) which contains five series of peaks representative of amide (Table 1), intermediate amide/cyclodehydrated (Table 3), and fully cyclodehydrated (Table 4) species. The dominant species observed are labeled as follows: series CCa represents amide species possessing carboxyl–carboxyl end groups (species 1–6); series

CCb identifies intermediate amide/cyclodehydrated species containing carboxyl–carboxyl end groups (species 3–6); and species 3–4 signifies intermediate amide/cyclodehydrated species containing carboxyl–amine end groups. The next most abundant species are cyclic amide structures (species 1–5), series Cyb (which identifies intermediate amide/cyclodehydrated cyclic structures—species 3–5), and series DAc (which represents cyclodehydrated species containing decarboxyl–amine end groups—species 4–4). Less abundant intermediate amide/cyclodehydrated species contain the following end groups (in their observed order of abundance): species representative of carboxyl–carboxyl end group adduct formation with 3AQ

Table 5. Structural Assignments for Peaks in the MALDI-TOF Mass Spectra Reported in Figures 2 and 3<sup>a</sup>

Species	Structure (M)	300 °C Na <sup>+</sup> M (Da)
5-b1		<u>715.2</u> (n = 1, m = 2)... <u>2840.7</u> (n = 10, m = 2)
5-b2		<u>759.2</u> (n = 1, m = 2)... <u>995.3</u> (n = 2, m = 2)
5-b3		<u>695.2</u> (n = 1, m = 1)... <u>1167.3</u> (n = 3, m = 1)
5-b4		<u>873.2</u> (n = 2, m = 1)... <u>1345.4</u> (n = 4, m = 1) <u>891.2</u> (n = 1, m = 2)... <u>1363.4</u> (n = 3, m = 2)
5-b5		<u>567.2</u> (n = 0, m = 2), <u>803.2</u> (n = 1, m = 2)... <u>2928.8</u> (n = 10, m = 2)

<sup>a</sup> Right-hand column has the same information as Table 1.

(species 3–7) and its associated decarboxylated species (species 3–10), carboxyl-amine (species 3–2) along with its amide (series CAA—species 1–2) and cyclodehydrated (species 4–2) species, followed by a species representative of carboxyl-amine adduct formation with 3AQ (species 3–3). Minor quantities of intermediate amide/cyclodehydrated species contain decarboxyl-decarboxyl (species 3–11) and decarboxyl-carboxyl (species 3–9) end groups. Overall, this figure displays a predominance of linear species with an increase in cyclic structures and species containing decarboxylated end groups (with respect to Figure 1). Observed species (Tables 3 and 4) indicate that the cyclodehydration process is well underway at 250 °C.

Figure 3 shows a PBO-amine precursor mass spectrum (after curing at 300 °C for 45 min) ( $M_w = 1580$  g/mol) which contains fully cyclodehydrated species. Three distinct series of peaks are labeled in this figure (in order of abundance): series DAc is representative of decarboxyl-amine end groups (species 4–4); series CAC identifies species containing carboxyl-amine end groups (species 4–2); and series CCc represents carboxyl-carboxyl end groups (species 4–6). Species 4–3 (an abundant species not belonging to a series) is representative of carboxyl-amine adduct formation with 3AQ. Species of very low abundance contain decarboxyl-carboxyl (species 4–9) and decarboxyl-decarboxyl (species 4–11) end groups along with the cyclic and branched species. This figure displays an overall predominance of linear species with very minor quantities of cyclic (species 4–5) and branched species (Table 5) present.

Comparison of the MALDI-TOF mass spectra displayed in Figures 1–3 reveals a decrease in weight-average molecular mass upon full cyclodehydration, from 2180 (Figure 1) to 1580 g/mol (Figure 3), and a shift from the carboxyl-carboxyl dominated end groups in Figures 1 (series CCA and CQA) and 2 (series CCA and CCb) to an overall predominance of decarboxyl-amine end groups (series DAC), as displayed in Figure 3. The observed shift in end groups and decrease in average molecular mass indicate that chain rupture is occurring in the cyclodehydration process.

Figure 4 displays a PBO precursor mass spectrum ( $M_w = 1770$  g/mol) containing four predominant series, labeled in order of abundance. There series are listed as follows: series CCA represents species containing of carboxyl-carboxyl end groups (species 6–6); series QQA and CQA identify species representative of carboxyl-carboxyl end groups after adduct formation with the 3AQ MALDI matrix (species 6–7 and 6–8); and series BQA labels branched species (species 6-b1). Less abundant species observed (in order of abundance) contain the following end groups: carboxyl-amine (species 6–2) along species representative of carboxyl-amine adduct formation with 3AQ (species 6–3); cyclic structures (species 6–5); and decarboxyl-carboxyl (species 6–9). This figure exhibits an overall predominance of linear species with minor branching (Table 6, species 6b-1). The abundances of the observed end groups are what would be expected for a synthesis using a very slight excess of diacid chloride monomer. The increased branching



Table 6. Structural Assignments for Peaks in the MALDI-TOF Mass Spectra Reported in Figures 4 and 5<sup>a</sup>

Species	Structure (M)	No Heat Na <sup>+</sup> M (Da)	250 °C Na <sup>+</sup> M (Da)
6-1		703.2 (n = 2), 973.2 (n = 3)... 2864.7 (n = 10)	
6-2		581.1 (n = 2), 851.2 (n = 3)... 1932.4 (n = 7)	581.1 (n = 2), 851.2 (n = 3)... 1391.3 (n = 5)
6-3		707.2 (n = 2), 977.2 (n = 3)... 2058.3 (n = 7)	707.2 (n = 2), 977.2 (n = 3)... 1517.4 (n = 5)
6-4		537.1 (n = 1), 807.2 (n = 2)... 2968.7 (n = 10)	537.1 (n = 1), 807.2 (n = 2)... 1347.3 (n = 4)
6-5		563.1 (n = 2), 833.2 (n = 3)... 2994.7 (n = 11)	563.1 (n = 2), 833.2 (n = 3)... 1373.3 (n = 5)
6-6		729.1 (n = 2)... 2890.6 (n = 10)	729.1 (n = 2)... 1539.3 (n = 5)
6-7		585.1 (n = 1), 855.2 (n = 2)... 3016.7 (n = 10)	585.1 (n = 1), 855.2 (n = 2)... 1395.3 (n = 4)
6-8		711.2 (n = 1)... 2332.6 (n = 7)	711.2 (n = 1)... 1521.4 (n = 4)
6-9		685.2 (n = 2), 955.2 (n = 3)... 2846.6 (n = 10)	685.2 (n = 2), 955.2 (n = 3)... 1495.3 (n = 5)
6-10		541.2 (n = 1), 811.2 (n = 2)... 2432.6 (n = 8)	541.2 (n = 1), 811.2 (n = 2)... 1351.3 (n = 4)
6-b1		859.2 (n = 0)... 2750.6 (n = 7)	859.2 (n = 0)... 1399.3 (n = 2)

<sup>a</sup> Right-hand columns have the same information as Table 1.

observed in the PBO precursor spectrum with respect to the PBO-amine precursor spectrum is to be expected due to the extra hydroxy pendant groups present on the PBO precursor oligomer backbone.

Figure 5 displays a PBO precursor mass spectrum (after curing at 250 °C for 45 min) ( $M_w = 1590$  g/mol) which contains amide (Table 6), intermediate amide/benzoxazole (Table 7), and fully cyclodehydrated (benzoxazole) species (Tables 8 and 9). The most abundant species are identified in four distinct series: series CCa represents amide species containing of carboxyl-carboxyl end groups (species 6-6); series QQa and CQa identify amide species representative of carboxyl-carboxyl end groups after adduct formation with the 3AQ MALDI matrix (species 6-7 and 6-8); and series CCb labels intermediate

amide/benzoxazole species containing carboxyl-carboxyl end groups (species 7-4). Observed species of low abundance contain the following end groups (in order of abundance): carboxyl-amine (intermediate species 7-2); decarboxyl-amine (intermediate species 7-3); benzoxazole branched structures (Table 9); amide cyclic structures (species 6-5); decarboxyl-carboxyl (intermediate species 7-6 and benzoxazole species 8-6); and amide species representative of carboxyl-amine adduct formation with 3AQ (species 6-3). This figure displays an overall predominance of linear species with a noticeable increase in species containing decarboxylated end groups (with respect to Figure 4); observed species (Tables 7 and 8) indicate that the cyclodehydration process is well underway at 250 °C.

Table 7. Structural Assignments for Peaks in the MALDI-TOF Mass Spectra Reported in Figure 5<sup>a</sup>

Species	Structure (M)	250 °C Na <sup>+</sup> M (Da)
7-1		685.2 (n = 1, m = 1), 955.2 (n = 2, m = 1)... 2036.5 (n = 6, m = 1)
7-2		563.1 (n = 1, m = 1), 833.2 (n = 2, m = 1)... 1914.4 (n = 6, m = 1) 545.1 (n = 1, m = 2), 815.2 (n = 2, m = 2)... 1355.3 (n = 4, m = 2) 527.1 (n = 1, m = 3), 797.2 (n = 2, m = 3)... 2148.5 (n = 7, m = 3) 509.1 (n = 1, m = 4), 779.2 (n = 2, m = 4)... 1589.3 (n = 5, m = 4)
7-3		789.2 (n = 1, m = 1)... 1059.3 (n = 2, m = 1)
7-4		711.1 (n = 1, m = 1), 981.2 (n = 2, m = 1)... 2062.4 (n = 6, m = 1) 693.1 (n = 1, m = 2), 963.2 (n = 2, m = 2)... 2044.4 (n = 6, m = 2) 945.2 (n = 2, m = 3)... 2026.4 (n = 6, m = 3) 927.2 (n = 2, m = 4)... 2008.4 (n = 6, m = 4)
7-5		837.2 (n = 1, m = 1)... 1377.3 (n = 3, m = 1)
7-6		667.1 (n = 1, m = 1), 937.2 (n = 2, m = 1)... 2018.4 (n = 6, m = 1) 649.1 (n = 1, m = 2), 919.2 (n = 2, m = 2)... 1730.4 (n = 5, m = 2)
7-7		793.2 (n = 1, m = 1)... 1333.3 (n = 3, m = 1) 775.2 (n = 1, m = 2)... 1585.4 (n = 4, m = 2) 757.2 (n = 1, m = 3)... 1567.4 (n = 4, m = 3)
7-8		909.2 (n = 2, m = 1)... 1377.2 (n = 4, m = 1)

<sup>a</sup> Right-hand column has the same information as Table 1.

Figure 6 shows a PBO precursor mass spectrum (after curing at 300 °C for 45 min) ( $M_w = 1550$  g/mol) which contains fully cyclodehydrated (benzoxazole) species with two predominate series of peaks. Series BCc identifies branched species containing carboxyl end groups (species 9-b5) and series BDc represents branched species with carboxyl and decarboxylated end groups (species 9-b6). Branched species (Table 9) dominate this figure with small quantities of linear species present representing the following end groups (in their order of abundance): decarboxyl-carboxyl (species 8-6); species representative of decarboxyl-carboxyl and carboxyl-carboxyl

adduct formation with 3AQ (species 8-7 and 8-5); decarboxyl-aldehyde (species 8-8); and cyclic structures (species 8-3).

Comparing Figures 4-6, the MALDI-TOF mass spectra identify a slight decrease in weight-average molecular mass upon full cyclodehydration, from 1770 (Figure 4) to 1550 g/mol (Figure 6), and a shift from linear species in Figures 4 (series CCa, QQa, and CQa) and 5 (series CCb) to an overall predominance of branched structures in Figure 6 (series BCc and BDc). These changes are further indications of chain rupture occurring in the cyclodehydration process. PBO fibers display the ability to compensate for mass loss (from chain rupture)

Table 8. Structural Assignments for Peaks in the MALDI-TOF Mass Spectra Reported in Figures 5 and 6<sup>a</sup>

Species	Structure (M)	250 °C Na <sup>+</sup> M (Da)	300 °C Na <sup>+</sup> M (Da)
8-1		527.1 (n = 1), 761.2 (n = 2)... 1229.2 (n = 4)	527.1 (n = 1), 761.2 (n = 2)... 1932.3 (n = 7)
8-2		653.2 (n = 1), 887.2 (n = 2)... 1121.2 (n = 3)	653.2 (n = 1), 887.2 (n = 2)... 1590.3 (n = 5)
8-3		725.1 (n = 3)... 1193.2 (n = 5)	725.1 (n = 3)... 1427.2 (n = 6)
8-4		657.1 (n = 2), 891.2 (n = 3)... 1359.2 (n = 5)	657.1 (n = 2), 891.2 (n = 3)... 1594.3 (n = 6)
8-5		549.1 (n = 1), 783.2 (n = 2)... 1486.3 (n = 5)	549.1 (n = 1), 783.2 (n = 2)... 2656.5 (n = 10)
8-6		613.1 (n = 2), 843.2 (n = 3)... 1550.3 (n = 6)	613.1 (n = 2), 843.2 (n = 3)... 1081.2 (n = 4)
8-7		505.1 (n = 1), 739.2 (n = 2)... 973.2 (n = 3)	505.1 (n = 1), 739.2 (n = 2)... 2144.4 (n = 8)
8-8		597.0 (n = 1), 831.2 (n = 2)... 1299.1 (n = 4)	597.0 (n = 1), 831.2 (n = 2)... 2470.3 (n = 9)

<sup>a</sup> Right-hand columns have the same information as Table 1.

through the formation of branched structures, while PBO-amide fibers experience greater mass loss due to their limited ability of form branched structures. Finally, it should also be noted that the PBO spectra (Figures 4–6) do not exhibit a shift from carboxyl-carboxyl to carboxyl-amine end groups, as observed in the PBO-amide spectra (Figures 1–3).

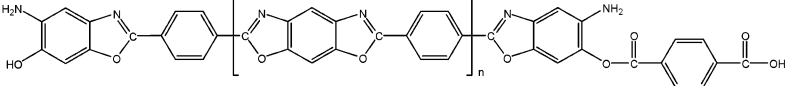
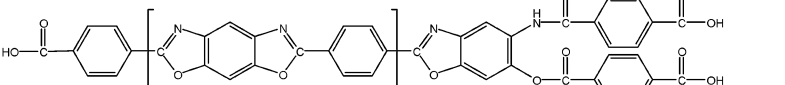
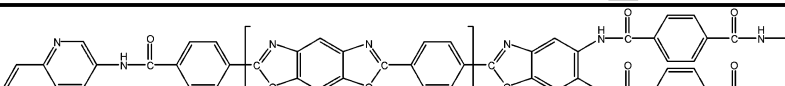
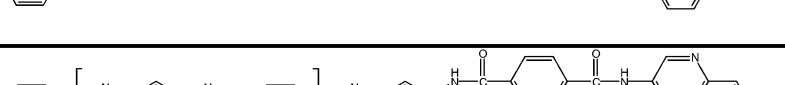
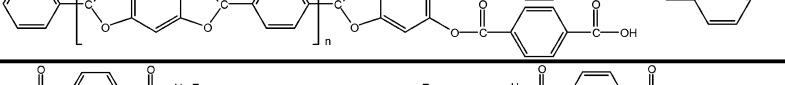
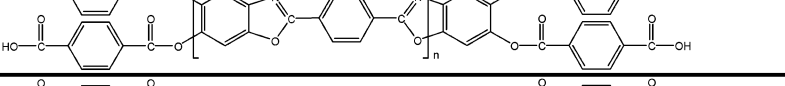
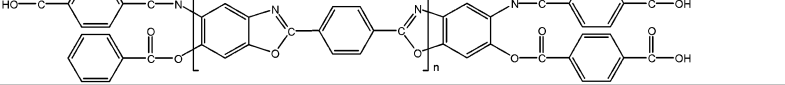
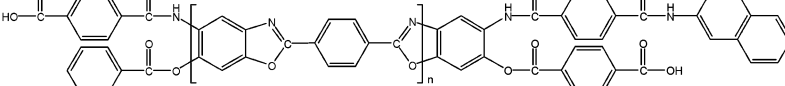
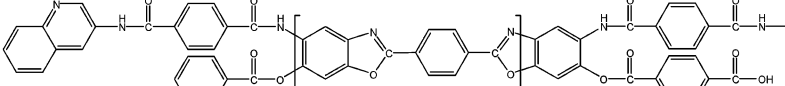
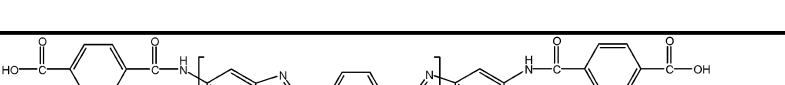
Figure 7 exhibits two graphs displaying evolved gases (species 1, 2, and 3) from the curing process (100–300 °C) of PBO-amide (Figure 7a) and PBO (Figure 7b) precursors. Species 1 represents 4-cyanobenzoic acid, species 2 identifies terephthalic acid (hydrolyzed diacid chloride monomer), and species 3 labels 2-benzoic acid-benzoxazole. Structures of these species are displayed in Table 10. Appreciable amounts of volatilized materials were first detected at a curing temperature of 250 °C with the observation of species 2 (97K counts—7a and 92K counts—7b) with very small quantities of species 1, indicative of chain rupture (6K counts—7a and 6K counts—7b). At 275 °C large quantities (398K counts—7a and 383K counts—7b) of species 2 were detected along with increasing amounts (27K counts—7a and 26K counts—7b) of species 1. The final heating at 300 °C brought about a large evolution of species 1 (93K counts—7a and 85K counts—7b), species 2 (907K counts—7a and 824K counts—7b), and species 3 (998K counts—7a and 779K counts—7b), which coincided with the increased branching detected in the MALDI-TOF mass spectra at this curing temperature. Furthermore, the larger abundance of species 3 in Figure 7a (with respect to 7b) coincides with the PBO-amide MALDI-TOF mass spectra (Figures 1–3) displaying a greater decrease in average molecular weight than the PBO MALDI-

TOF mass spectra (Figures 4–6). Since greater mass loss is occurring, we would expect to observe more fragment peaks, such as species 3. TGA data of the PBO-amide and PBO precursors also showed similar weight losses up to 300 °C, which further validated our MALDI-TOF MS and EGA/GC/MS findings. These EGA/GC/MS data indicate that mass loss (from chain rupture) and evolution of low mass material lead to branching. Experimental data indicates that branched species are formed when low molecular weight materials are volatilized above 200 °C and are not due to the evaporation-grinding MALDI-TOF MS sample preparation method. These volatile materials have the potential to react with the PBO and PBO-amide precursors; introducing branch points which limit the cyclodehydration process.

## Conclusions

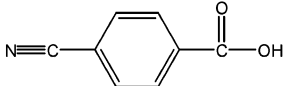
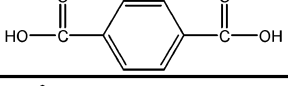
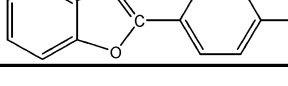
The combination of MALDI-TOF MS and EGA/GC/MS was successfully exploited to follow the cyclodehydration of PBO and PBO-amide precursor fibers. Findings indicate that fully cured PBO fibers convert from predominately linear species to predominately branched species, with minor reductions in average molecular weight. Fully cured PBO-amide fibers retained linear species as the predominant product (with only minor branching observed) but exhibited significant reductions in average molecular weight. Cured PBO-amide (300 °C) fibers show a significant increase in decarboxylated end groups as well as a shift from carboxyl-carboxyl to carboxyl-amine end groups. Intermediate species observed during the curing process of both fibers identify critical

Table 9. Structural Assignments for Peaks in the MALDI-TOF Mass Spectra Reported in Figures 5 and 6<sup>a</sup>

Species	Structure (M)	250 °C Na <sup>+</sup> M (Da)	300 °C Na <sup>+</sup> M (Da)
9-b1		545.1 (n = 1), 779.2 (n = 2)... 1247.2 (n = 4)	545.1 (n = 1), 779.2 (n = 2)... 1481.3 (n = 5)
9-b2		589.1 (n = 1), 823.2 (n = 2)... 1057.2 (n = 3)	589.1 (n = 1), 823.2 (n = 2)... 2228.4 (n = 8)
9-b3		607.2 (n = 0), 841.2 (n = 1)... 1309.3 (n = 3)	607.2 (n = 0), 841.2 (n = 1)... 1543.3 (n = 4)
9-b4		671.2 (n = 1), 905.2 (n = 2)... 1373.3 (n = 4)	671.2 (n = 1), 905.2 (n = 2)... 2076.4 (n = 7)
9-b5		755.1 (n = 1)... 1223.2 (n = 3)	755.1 (n = 1)... 2394.4 (n = 8)
9-b6		711.1 (n = 1), 945.2 (n = 2)... 1413.3 (n = 4)	711.1 (n = 1), 945.2 (n = 2)... 2116.4 (n = 7)
9-b7		837.2 (n = 1)... 1071.2 (n = 2)	837.2 (n = 1)... 1305.3 (n = 3)
9-b8		729.2 (n = 0)... 2134.5 (n = 6)	729.2 (n = 0)... 2134.5 (n = 6)
9-b9		667.1 (n = 2), 901.2 (n = 3)... 1369.3 (n = 4)	667.1 (n = 2), 901.2 (n = 3)... 1838.3 (n = 6)
9-b10		793.2 (n = 1)... 1730.4 (n = 5)	793.2 (n = 1)... 1730.4 (n = 5)

<sup>a</sup> Right-hand columns have the same information as Table 1.

Table 10. Structural Assignments for Peaks in the EGC/GC/MS Chromatogram Reported in Figure 7

Species	Structure (M)
1	
2	
3	

temperatures in the cyclodehydration, branching, and decarboxylation processes. Around 250 °C the cyclodehydration

process is noticeably occurring and (at temperatures of 275 °C and above) decarboxylation and branching become more pronounced with increasing temperatures.

Results of this study indicate that a combination of MALDI-TOF MS and EGA/GC/MS has great potential for examination of thermal, chemical, and photodegradation pathways of high molecular weight condensation polymers. Studies are currently underway to validate these assumptions.

**Acknowledgment.** We would like to thank Charles M. Lukehart and Jiang Li for supplying the TGA information used in this study and William K. Nonidez for use of his Py-GC/MS instrument.

## References and Notes

- (1) Yang, H. H. *Aromatic High-Strength Fibers*; John Wiley & Sons: New York, 1989.

- (2) Chang, J.-H.; Chen, M. J.; Farris, R. J. *Polymer* **1998**, *39*, 5649.
- (3) Johnson; Mathias. *J. Polym. Sci., Part A: Polym. Chem.* **1995**, *33*, 1901.
- (4) Evers, R. C.; Arnold, F. E.; Helminiak, T. E. *Macromolecules* **1981**, *14*, 925.
- (5) Choe, E. W.; Kim, S. N. *Macromolecules* **1981**, *14*, 920.
- (6) Montaudo, G.; Lattimer, R. P. *Mass Spectrometry of Polymers*; CRC Press: Boca Raton, FL, 2001.
- (7) Ji, H.; Nonidez, W. K.; Mays, J. W.; Advincula, R. *Macromolecules* **2005**, *38*, 9950.
- (8) Reisch, M. S. *Chem. Eng. News* **2005**, *83*, 18.
- (9) Gies, A. P.; Nonidez, W. K. *Anal. Chem.* **2004**, *76*, 1991.
- (10) Gies, A. P.; Nonidez, W. K.; Anthamatten, M.; Cook, R. C. *Macromolecules* **2004**, *37*, 5923.
- (11) Gies, A. P.; Nonidez, W. K.; Anthamatten, M.; Cook, R. C.; Mays, J. W. *Rapid Commun. Mass Spectrom.* **2002**, *16*, 1903.
- (12) Sillion, B.; Mercier, R.; Picq, D. In *Synthetic Methods in Step-Growth Polymers*; Rodgers, M. E., Long, T. E., Eds.; John Wiley & Sons: Hoboken, NJ, 2003; p 316.

MA060038H